frontiers | Frontiers in Chemistry

TYPE Original Research
PUBLISHED 02 November 2022
DOI 10.3389/fchem.2022.1046058

OPEN ACCESS

EDITED BY
Runping Ye,
Nanchang University, China

REVIEWED BY
Gang Feng,
Nanchang University, China
Xiaobing Yang,
Wuyi Unviersity, China

*CORRESPONDENCE
Zaiku Xie,
xzk@sinopec.com
Zhicheng Liu,
liuzc.sshy@sinopec.com

SPECIALTY SECTION
This article was submitted to Catalytic Reactions and Chemistry, a section of the journal Frontiers in Chemistry

RECEIVED 16 September 2022
ACCEPTED 10 October 2022
PUBLISHED 02 November 2022

CITATION
He L, Wang Y, Wang C, Liu Z and Xie Z (2022), Pyridinic nitrogen dominated doping on Pd/carbon catalysts for enhanced hydrogenation performance. *Front. Chem.* 10:1046058. doi: 10.3389/fchem.2022.1046058

Pyridinic nitrogen dominated doping on Pd/carbon catalysts for enhanced hydrogenation performance

Limin He[1], Yangdong Wang[1], Can Wang[1], Zhicheng Liu[1]* and Zaiku Xie[2]*

[1]State Key Laboratory of Green Chemical Engineering and Industrial Catalysis, Shanghai Research Institute of Petrochemical Technology, SINOPEC Corp, Shanghai, China, [2]China Petrochemical Corporation (SINOPEC Group), Beijing, China

The hydrogenation of 4-carboxylbenzaldehyde over Pd catalysts is a crucial process during the production of pure terephthalic acid. Herein, ZIF-8 derived carbon materials (NC) with adjustable N types were synthesized and used as the supports of Pd catalysts. Pd supported on NC with 50.5% of pyridinic N exhibited best hydrogenation activity with a TOF value of 4.1 min^{-1}. The microstructures of NC support and electronic structures of Pd in Pd/NC were investigated by techniques such as XRD, N_2 physisorption, XPS, H_2-O_2 titration and TEM. The nitrogen species in CN surface not only can adjust chemical state and dispersion of Pd nanoparticles (NPs), but also promote the adsorption and activation capability of H_2 molecular. Besides, the ratio of Pd^0/Pd^{2+} and Pd dispersion were closely correlated with pyridinic nitrogen content. The improvement in hydrogenation activity and stability of Pd/CN catalyst in relative to Pd/C were ascribed to the synergistic effect of pyridinic nitrogen and active site Pd^0.

KEYWORDS

hydrogenation, pallidium, carbon materials, pyridinic nitrogen, synergistic effect

Introduction

Terephthalic acid (TA) as an important intermediate was widely used for the manufacture of polyethylene terephthalate. Industrially, 4-carboxy benzaldehyde (4-CAB) was the main impurities of crude terephthalic acid. The remove of 4-CBA was conducted by the catalytic hydrogenation of 4-CBA to obtain p-toluic acid over Pd catalysts. (Jhung et al., 2002). So far, activated carbon supported Pd catalysts remain the most efficient catalyst in actual industrial applications (Menegazzo et al., 2007; Zhu et al., 2015). Nevertheless, the stability of Pd/C is not satisfactory and the aggregation of Pd NPs is severe due to the weak interaction of Pd and carbon. As is well known, the nature of the supports played a strong influence on the structural properties of Pd catalysts and their catalytic hydrogenation performance. So far, various materials such as SiO_2 (Li et al., 2008), SiC (Zhou et al., 2012; Tie et al., 2018), TiO_2 (Kan et al., 2012; Liu et al., 2018) and carbon materials (Wang et al., 2015; Li et al., 2018) were applied as the supports of Pd for the catalytic hydrogenation of 4-CBA. Among various supports, carbon

materials were still ideal supports of Pd due to their good corrosion resistance, excellent thermal stability and good chemical inertness (Wang et al., 2022; Zhou et al., 2022). Recently, nitrogen doped material demonstrated fantastic catalytic performance in various fields (Siuzdak et al., 2015; Wang et al., 2017; Wang et al., 2019; Lobiak et al., 2020; Shi et al., 2020), especially in the heterogeneous catalytic hydrogenations or oxidations (Xu et al., 2012; Lu et al., 2019; Hao et al., 2021; Wang et al., 2021). The incorporation of nitrogen atoms into carbon materials or metal oxide had a significant impact on the chemical and electronic properties of metal catalysts, such as dispersion and electronic densities of metal nanopaticle, chemical state, active sites, etc (Cui et al., 2016; Shen et al., 2020; Mao et al., 2019; von Deak et al., 2012; Wood et al., 2014). In early study, Wilson et al. reported the introduction of amine groups in stone-fruit activated carbon can increase the proportion of Pd^0, resistant to re-oxidation (Radkevich et al., 2008). In contrast, Xia et al. revealed that pyridinic or pyrrolic nitrogen atoms showed strong interact with Pd, leading to the high proportion of $Pd^{\delta+}$ species over nitrogen doped Pd catalysts (Jiang et al., 2016)). Bulusheva et al. synthesized Pd catalysts supported on nitrogen functionalized mesoporous carbon, and confirmed that the surface concentration of Pd^0 decreased after N doping (Bulushev et al., 2016). Besides, nitrogen doped activated carbon synthesized with dicyandiamide as nitrogen source and as supports of Pd catalysts (Nie et al., 2016), the percentage of Pd^0 decreased obviously from 78.6% to 15.5% and then increased to 27.7%. Generally, nitrogen dopant in carbon materials mainly existed four types. They were pyridinic N, pyrrolic N, graphitic N, and N-oxide respectively (Yang et al., 2014; Cao et al., 2017; Podyacheva et al., 2017). Because of the complicacy of different types of N doping, the effects of nitrogen doping on the electronic states of metal catalysts have remained elusive and no consensus.

In our previous work (He et al., 2021), we introduced nitrogen atoms into activated carbon to stabilize Pd NPs and adjust their chemical and electronic structure using urea as nitrogen resource. The ZIF-8 framework, which has uniform ordered pore structure and rich nitrogen element, was an ideal nitrogen resource to prepare nitrogen doped materials by calcination under an N_2 atmosphere. Inspired by these results, AC@ZIF-8 hybrid nanocomposites were prepared by the growth of ZIF nanocrystals on the surface of AC. And then, a series of nitrogen doped carbon materials (NC) with adjustable N types and N contents have been synthesized by the carbonization of ZIF-8 based carbon materials. Pd on different NC samples were also synthesized and tested for the hydrogenation of 4-CBA under mild reaction conditions. The effects of nitrogen doping on the structural and electronic properties of NC supports and Pd/NC catalysts were investigated by XRD, N_2 physisorption, XPS, H_2-O_2 titration and TEM. The relationship between nitrogen doping and its impacts on hydrogenation performance of Pd/NC catalysts are discussed in detail.

Experimental section

Materials

All chemical agents were commercially available. They were used without further purification. The reactant 4-CBA were obtained from Aladdin Chemical Reagent (Shanghai, China). Palladium chloride was purchased from Sigma-Aldrich. Activated carbon was provided by Sinopec Shanghai Petrochemical Company Limited. Zinc nitrate hexahydrate, 2-methylimidazole, phosphoric acid (H_3PO_4, 85 wt% in H_2O), ammonia solution ($NH_3 \cdot H_2O$, 25 wt% in H_2O) were purchased from Sinopharm Chemical Reagent Co., Ltd.

Synthesis of NC samples

Firstly, ZIF-8 was supported on AC according to the previous report with few modifications (Li J. et al., 2016). Typically, the activated carbon (C) was dispersed in the solution of 0.6 g $Zn(NO_3)_2{\cdot}6H_2O$ with 8 ml ethanol and 2 ml water. 1.31 g 2-methylimidazole dissolved in the mixture of 8 ml ethanol and 2 ml water. Then the solution of 2-methylimidazole was added into the above salt solution with stirring for 20 min. The mixed solution was transferred into a 100 ml Teflon-lined stainless autoclave. After sealed, the autoclave was heated to 120°C and maintained for 2 h. The hydrothermal product was filtered and washed thoroughly by water, and finally dried at 110°C. The above obtained samples (C@ZIF-8) were carbonized at different temperatures (500°C, 600°C, 700°C, and 800°C) for 2 h in nitrogen atmosphere. The carbonized samples were treated by HCl aqueous solution and washed by water. After drying at 120°C, the final samples were denoted as NC-T, where T represented the calcination temperature of 500°C, 600°C, 700°C, and 800°C.

Preparation of Pd/NC catalysts

The Pd catalysts was prepared by an impregnation method using aqueous solution of $PdCl_2$. The theoretical loading contents of Pd on NC samples were 0.5 wt%. The Pd catalysts were denoted as Pd/NC-T, in which T represented 500°C, 600°C, 700°C, and 800 C. For comparison, activated carbon without nitrogen doping supported Pd catalyst (Pd/C) was also prepared with the same method as described above.

Materials characterization

Powder X-ray diffraction (XRD) measurement was carried out using Bruker D8 Advance diffractometer, with Cu Kα radiation (g = 0.15406 nm) at step scan 0.02° from 5° to 80°. The nitrogen adsorption/desorption isotherms were obtained at 77 K on a Micromeritics ASAP 2020 analyzer. The total porous volume (V_{total}) was estimated from the adsorbed capacity of

nitrogen at a relative pressure P/P_0 of 0.98. The microporous volume (V_{micro}) was determined using the t-plot method. X-ray photoelectron spectroscopy (XPS) analysis was performed with an AXIS Ultra DLD photoelectron spectrometer (Kratos Analytical, United Kingdom) using monochromatic Al Kα radiation. The C1s peak at 284.6 eV was applied as reference to calibrate the position of the other peaks. Palladium dispersion on NC samples were tested by hydrogen titration of chemisorbed oxygen (H_2-O_2 titration) in a Micromeritics Autochem II 2920 instrument with a thermal conductivity detector (TCD). Before the tests, the Pd catalysts were firstly reduced under a hydrogen atmosphere at 200°C for 60 min. Typically, 400 mg catalyst sample was pre-reduced at 200°C by hydrogen for 120 min. After pre-reduction, hydrogen absorbed on the surface of catalyst was titrated by 15 pulses of oxygen until full saturation. Furthermore, the resulting monolayer of adsorbed oxygen was titrated using 15 pulses of hydrogen until constant TCD signal detected. The content of Pd loading was tested by an inductively coupled plasma emission spectrometer (ICP-OES, Varian 725ES). The hydrogen temperature programmed desorption (H_2-TPD) experiments was carried out using a Micromeritics Autochem II 2920 instrument equipped with a thermal conductivity detector (TCD). HRTEM images and elemental mapping of Pd catalysts were conducted on a Tecnai 20 S-TWIN electron microscope operated at 200 kV.

Catalytic hydrogenation tests

The Hydrogenation of 4-CBA was performed in a 100 ml stainless autoclave with a Teflon liner. Generally, 50 mg catalyst and 0.15 g 4-CBA were dispersed in 50 ml de-ionized water. After the autoclave was sealed, it was purged by hydrogen to remove the air. Then it was pressured with 0.8 MPa hydrogen. Finally, the autoclave was heated to 80°C for hydrogenation reaction. After the completion of this reaction, the obtained liquid products were treated with 14% $NH_3{\cdot}H_2O$ and 17% H_3PO_4 aqueous solutions respectively. Finally, the liquid products were analyzed through high-performance liquid chromatography (HPLC, Agilent 1,200). The HPLC was equipped with a UV detector and a C-18 column (4.6*250 mm, 5 μm). The hydrogenation of 4-CBA over Pd catalysts leaded to primary product 4-hydroxymethyl benzoic acid. The TOF (turnover frequency) of Pd catalysts was calculated as the number of moles of 4-CBA converted per mole of Pd per minute.

Results and Discussion

Effects of nitrogen doping on the structure of NC supports

All of NC samples in present work were synthesized in similar procedure but at different calcination temperatures ranging from 500 to 800°C to tailor different N species. Firstly, XRD patterns of C@ZIF-8 and NC samples were shown in Figure 1. Before calciantion, the precursor C@ZIF-8 showed the diffraction of ZIF-8 (cubic space group), corresponding to the ZIF-8 (011) (002) and 112) diffractions, respectively (Zhang et al., 2014). After calcination at different temperature, four NC samples exhibited similar diffraction peaks at around 25° and 43°, corresponding to the graphitic carbon (002) and (100) diffraction peaks (Fu et al., 2017). Further, nitrogen adsorption-desorption isotherms of NC samples were tested and the structure parameters of these materials were summarized in Table 1. NC-500 exhibited the lowest BET surface area (678.1 m^2/g). NC-600 showed higher BET surface area (701.6 m^2/g) than that of NC-500. NC-700 and NC-800 have similar BET surface area with NC-600. These results

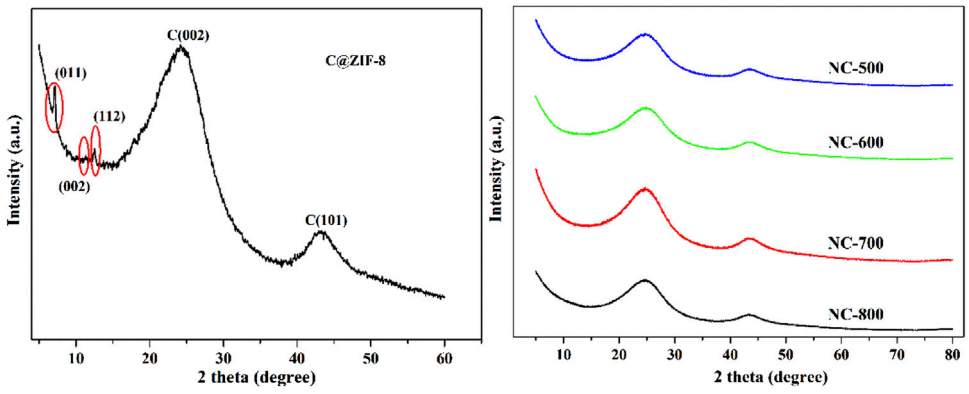

FIGURE 1
XRD spectra of ZIF-8-C-pre and NC samples.

TABLE 1 Summary of porosity parameters of NC samples.

Sample	S_{BET} (m^2/g)	S_{mic} m^2/g	V_t (cm^3/g)	V_{micro} (m^3/g)
NC-500	678.1	548.9	0.33	0.25
NC-600	701.6	552.2	0.34	0.25
NC-700	707.3	582.1	0.34	0.26
NC-800	704.1	614.1	0.32	0.28

The specific surface areas (S_{BET}) were calculatd by the Brunauer-Emmett-Teller (BET) method. V_t denoted the total pore volume. The micropore area (S_{mic}) and micropore volume (V_{micro}) was determined by t-plot method.

demonstrated that nitrogen species of NC can be regulated by different pyrolysis temperature at 600–800°C, while similar surface area and porous volume of NC were preserved.

XPS characterization was performed to analyze N types and N contents of NC samples (Peng et al., 2014; Fu et al., 2017; Yang et al., 2018). As shown in Figure 2, the high-resolution N1s XPS spectra of four NC samples revealed there were mainly three types of N species: pyridinic N (N1) at 398.5 eV, pyrrolic N (N2) at 399.8 eV and graphitic N at 401.9 eV (N3) (Xiong et al., 2014; Chen et al., 2015). The typical nitrogen types in nitrogen doped carbon materials were shown in Scheme 1 (Li M. et al., 2016; Cao et al., 2017; Quílez-Bermejo et al., 2019). In Figure 3, the total N content decreased from 2.58 to 2.19 at.% with the increasing of calcination temperature. The relative contents of different N species in Figure 3 were calculate based on the integration areas of each N1s peak component from the N1s XPS spectra in

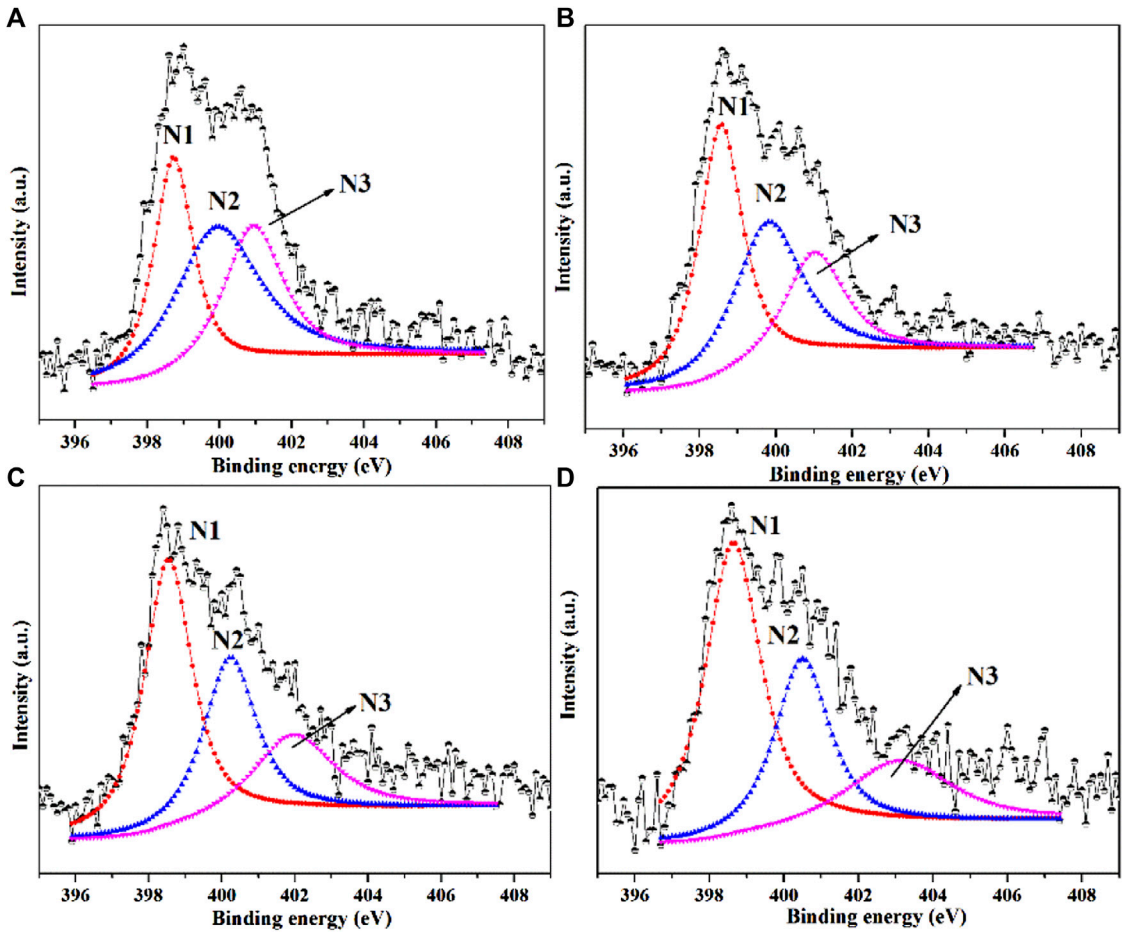

FIGURE 2
N 1s XPS spectra of **(A)** NC-500, **(B)** NC-600, **(C)** NC-700 and **(D)** NC-800. (N1: pyridinic N; N2: pyrrolic N; N3: graphitic N).

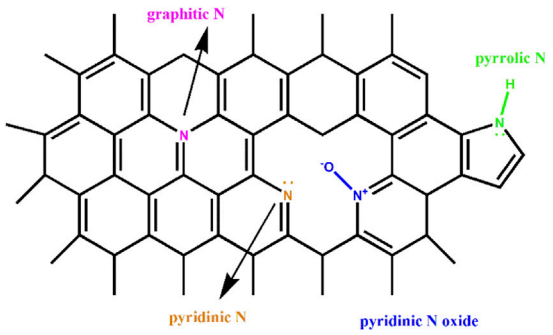

SCHEME 1
Nitrogen types in nitrogen doped carbon materials.

Figure 2. The relative percentage of pyridinic N increased from 30.5% to 50.5%. Differently, the percentage of pyrrolic N decreased continuously with increasing calcination temperature. Similar results have been reported earlier for N doping carbon materials, which revealed that pyrrol functional groups were not stable at high temperature and partly transformed to pyridinic N (Arrigo et al., 2008; Sun et al., 2017).

Effects of nitrogen doping on the electronic structure of Pd/NC catalysts

The influence of N doping on the electronic structures of Pd NPs was also studied by XPS. As shown in Figure 4, the four Pd 3d XPS spectra was fitted using four separated components with peaks at 335.8, 341.2, 337.3, and 342.5 eV. The former two peaks were ascribed to Pd^0 species (Pd^0 $3d_{5/2}$, Pd^0 $3d_{3/2}$). The latter two peaks were assignable to Pd^{2+} species (Pd^{2+} $3d_{5/2}$, Pd^{2+} $3d_{3/2}$) (Xu et al., 2012). As illustrated in Figure 5, the ratio of Pd^{2+} against Pd^0 (Pd^0/Pd^{2+}) gradually increased with the temperature of calcination from 500°C to 800°C. As revealed in Figure 5, the ratio of Pd^0/Pd^{2+} had only weak dependence on N content. However, the ratio of Pd^0/Pd^{2+} showed strong dependence on pyridinic N. This indicated that pyridinic N as preferential anchoring sites could favor the formation of high ratio of Pd^0/Pd^{2+} by donating electrons toward neighboring Pd nanoparticles.

Besides, Pd dispersion (D_{Pd}) was evidenced by H_2-O_2 titration analysis. As shown in Table 2, Pd/C showed the lowest Pd dispersion. However, NC as the supports of Pd nanoparticles exhibited well dispersed with D_{Pd} higher than 25%. Previous studies indicated that carbon materials with N doping favored well dispersion of metal nanoparticles compared to the un-doped ones (Shen et al., 2019; Hu et al., 2022). For example, Warczinski et al. has confirmed that loading of Pd on N-doped mesoporous carbon leaded to a better dispersion of Pd compared to those for Pd supported on N-free mesoporous carbon (Warczinski et al., 2020). In present work, N functional groups on the NC supports played a crucial role in effectively preventing the aggregation of PdNPs and anchoring the formed PdNPs.

Effects of nitrogen doping on the activity of Pd/NC

In order to elucidate the effect of N doping, the catalytic performances of Pd catalysts with and without N doping were

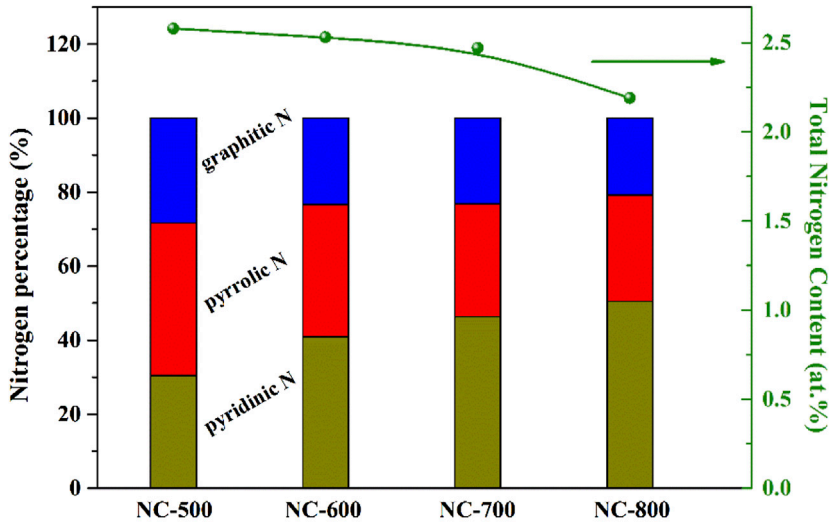

FIGURE 3
N contents and N types of different NC samples.

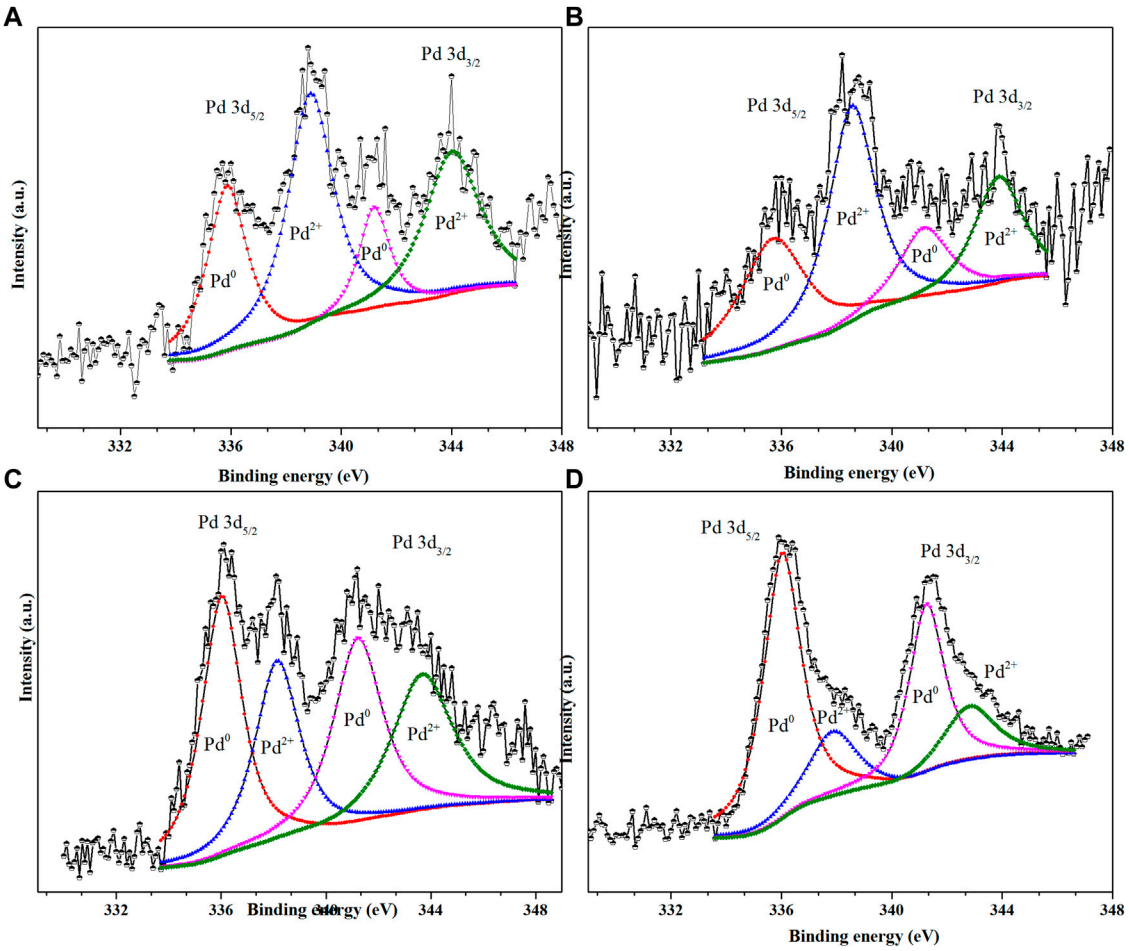

FIGURE 4
Pd 3d XPS spectra of **(A)** Pd/NC-500, **(B)** Pd/NC-600, **(C)** Pd/NC-700 and **(D)** Pd/NC-800.

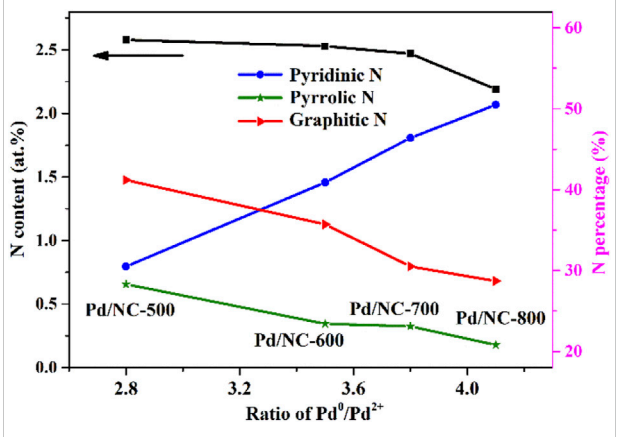

FIGURE 5
Relation of N content and N types with the ratio of Pd^0/Pd^{2+}.

TABLE 2 Physico-chemical properties of Pd catalysts.

Catalyst	Pd loading (wt%)	D_{Pd} (%)
Pd/C	0.40	21.3
Pd/NC-500	0.42	25.1
Pd/NC-600	0.41	25.3
Pd/NC-700	0.41	27.3
Pd/NC-800	0.42	32.6

investigated for the hydrogenation reaction of 4-CBA. As shown in Figure 6, activated carbon supported Pd catalyst (Pd/C) showed the lowest catalytic activity. The activity of Pd/NC-500 was higher than that of Pd/C. The activity of Pd/NC-600 and Pd/NC-700 further increased. The Pd/NC-800 showed highest TOF value of 4.1 min^{-1}. These catalytic

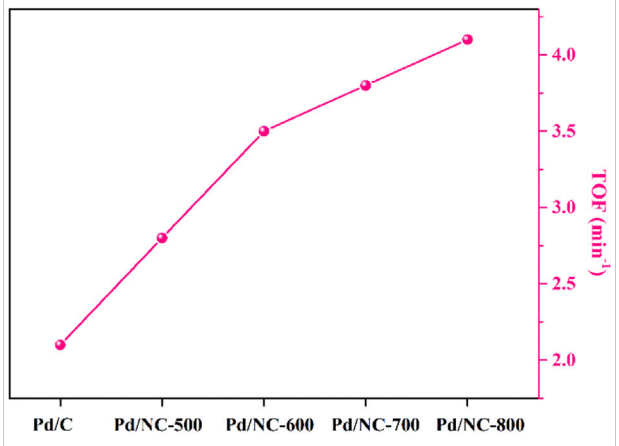

FIGURE 6
Catalytic performances of Pd catalysts for the hydrogenation of 4-CBA.

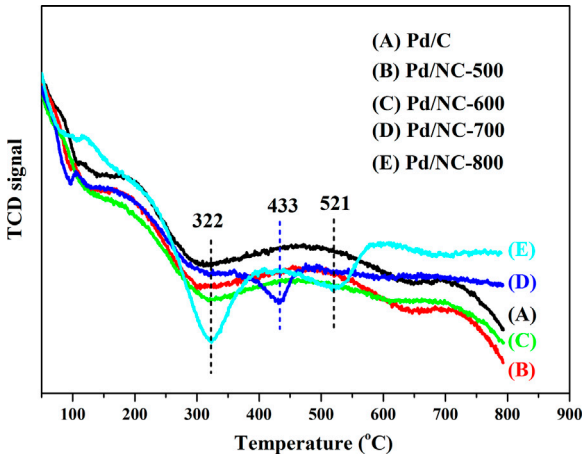

FIGURE 8
H_2-TPD spectra of **(A)** Pd/C, **(B)** Pd/NC-500, **(C)** Pd/NC-600, **(D)** Pd/NC-700 and **(E)** Pd/NC-800.

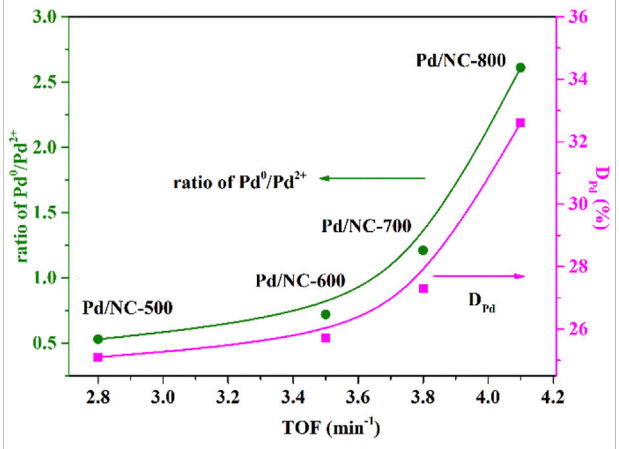

FIGURE 7
Dependence of D_{Pd} and Pd^0/Pd^{2+} on catalytic performance of Pd/NC.

results indicated TOF values (Figure 6) for the N-doped Pd catalysts were higher than Pd/C catalyst. The important promotion effects of N doping were further discussed as below.

Structure and activity relationship

The change of the ratio of Pd^0/Pd^{2+} was related with the different N content and N types of supports NC (Figure 5). As mentioned in Figure 3, the N content of NC decreased along with the increase of calcination temperature from 500°C to 800 C. However, the catalytic activities of Pd/NC increased with the increasing of calcination temperature (Figure 6). The variation trend of TOF value of Pd/NC did not agree with the effect of N content for 4-CBA hydrogenation. Thus, the N content was not the primary factor to influence hydrogenation activity, but the moderate N content may be a positive effect on this hydrogenation reaction. It was noticed that the ratio of Pd^0/Pd^{2+} in Pd/NC catalysts increased almost linearly along with the relative percentage of pyridinic N (Figure 5). The highest ratio of Pd^0/Pd^{2+} showed the best hydrogenation performance. Owing to its electron donating properties, pyridinic N can enhance the interaction between Pd and NC through its lone pairs as metal coordination sites, preventing the reoxidation of Pd^0. These results were in line with some experimental and DFT studies of pyridinic nitrogen strong interaction with metal nanoparticles (Li et al., 2016c; Nagpure et al., 2016; Jia et al., 2021). Besides, H_2-O_2 titration results indicated that Pd nanoparticles loading on NC supports maintained better dispersion compared with that of un-doped one.

To further clarify the important roles of nitrogen doping on catalytic activity of Pd/NC catalysts, the relationships of TOF of four Pd/NC catalysts and the ratio of Pd^0/Pd^{2+} as well as Pd dispersion were depicted in Figure 7. A strong dependence of the TOF of Pd/NC catalysts with the ratio of Pd^0/Pd^{2+} as well as Pd dispersion was observed. The higher the ratio of Pd^0/Pd^{2+}, the higher the catalytic activity of Pd/NC catalysts. Besides, the higher Pd dispersion also resulted in higher activity for Pd/NC catalysts. The above linear relationship may be attributed to the more exposure active sites Pd^0 over Pd/NC.

It was well known that the hydrogen dissociation/activation ability has a profound effect on catalytic hydrogenation performance (Liu et al., 2016; Bi et al., 2019). The H_2 activation/dissociation ability of Pd catalysts

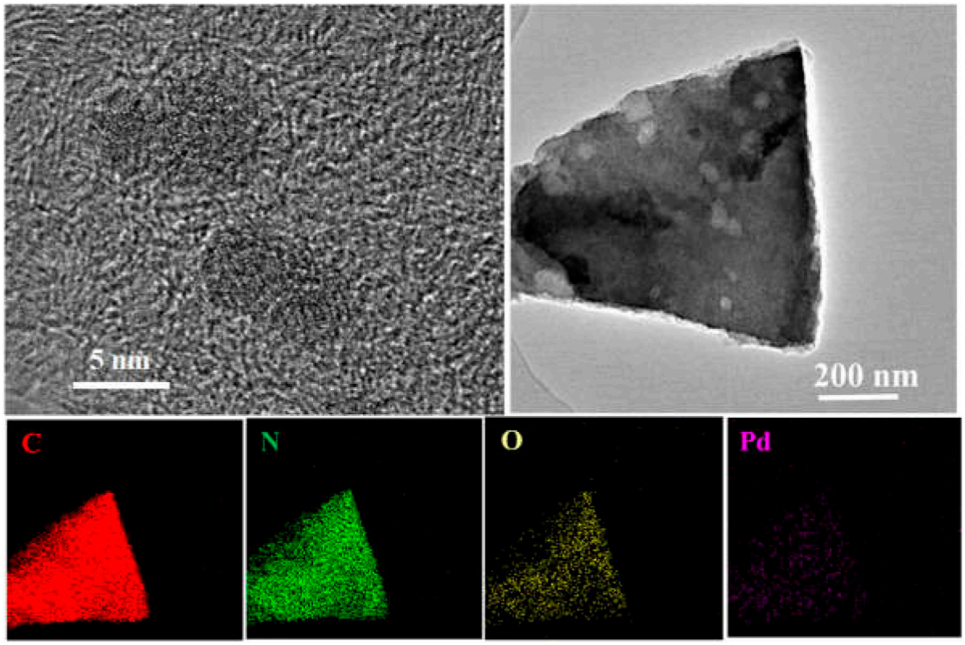

FIGURE 9
Representative HRTEM images of Pd/NC-800 and the EDS elemental mapping of C, N, O and Pd.

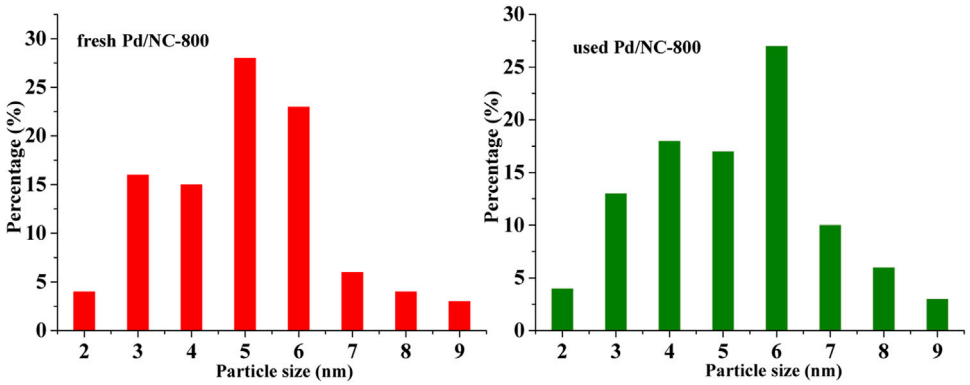

FIGURE 10
Particle size distributions of Pd NPs in fresh and used Pd/NC-800.

were studied *via* H_2-TPD. As shown in Figure 8, all catalysts showed a similar hydrogen desorption peak at 322°C, indicating that similar type of active sites existed on Pd catalysts surface. In addition, there was an obvious desorption peak at 433°C for Pd/NC-700. Pd/NC-800 showed two desorption peaks at low temperature of 322°C and high temperature of 521°C. The differences of desorption peaks indicated there were different types of active Pd sites on Pd/NC-700 and Pd/NC-800. The desorption peak at low 322°C was assigned to chemisorbed hydrogen on surface Pd active sites, and the high temperature peaks at 433 and 521°C were assigned to strongly chemisorbed hydrogen on different types of Pd active sites. Furthermore, the total hydrogen desorption of Pd/NC-800 were obviously larger than that of other Pd catalysts. Therefore, H_2-TPD results further concluded that the enhanced activation

capability of H_2 molecular in NPC-800 supported Pd catalyst also contributed to its higher hydrogenation activity. Furthermore, the morphologies of Pd NPs and the EDS elemental mapping of C, N, O and Pd of Pd/NC-800 was shown in Figure 9. It was evident that N and Pd were dispersed uniformly on the surface of Pd/NC-800. In addition, the used Pd/NC-800 catalyst was centrifuged and washed with ethanol for further TEM analysis. The particle size distributions of Pd in fresh and used Pd/NC-800 were shown in Figure 10. These results indicated that Pd nanoparticles in used Pd/NC-800 still maintained well dispersion and remained similar particle size distribution compared with that of fresh Pd/NC-800. In addition, Pd content in used Pd/NC-800 was also analyzed by ICP-OES technique. The results confirmed that the leaching of Pd was negligible. These results indicated Pd/NC-800 catalyst was quite stable. Therefore, the present NC materials can be promising catalyst supports to immobilize Pd nanoparticles (Li et al., 2013; Yu et al., 2021).

Conclusion

In summary, the present work demonstrated the comprehensive understanding of N doping on the catalytic activities of NC supported Pd catalysts for the catalytic hydrogenation of 4-CBA. The Pd/NC catalysts exhibited enhanced hydrogenation activity compared with Pd/C. Pd/NC-800 with 50.5% of pyridinic nitrogen exhibited excellent activity of 4.1 mim^{-1}. The excellent catalytic activity of Pd/NC-800 could ascribed to a high density of active species Pd^0 where the Pd^0 were confirmed to be mostly coordinated with pyridinic nitrogen. Furthermore, nitrogen species can also improve the dispersion of Pd NPs *via* strong interaction between Pd and pyridinic nitrogen. The Pd dispersion of Pd/NC-800 was up to 32.6%. Besides, the well dispersion of Pd nanoparticles can maintain even after reaction. Thus, pyridinic nitrogen species coordinated with active species Pd^0 also contributed to the high stability of Pd/NC catalysts. More importantly, the results of H_2-TPD tests clearly demonstrated that nitrogen species promoted the adsorption and activation capability of H_2 molecular. Particularly, H_2-TPD results also confirmed that new Pd active sites were created on the surface of Pd/NC catalysts. Therefore, the as-synthesized NC materials may be the promising supports of other supported metal catalysts, which are helpful for the dispersion and stabilization of metal nanoparticles.

Data availability statement

The original contributions presented in the study are included in the article/Supplementary Material, further inquiries can be directed to the corresponding authors.

Author contributions

LH prepared the catalysts, conducted the characterization analysis of catalysts, finished catalytic hydrogenation tests, analyzed the obtained experimental data and wrote the research paper. CW helped to discuss and analyze part of characterization results. YW contributed to thorough discussions and revision about this work. ZL and ZX supervised the project, helped to conceive the experiments, evaluated the data, and revised the manuscript. All authors participated in the discussion of the results of this manuscript.

Funding

This work was financially supported by the National Natural Science Foundation of China (project number: 91434102, U19B002) and the National Key R&D Program of China (2017YFB0702800).

Conflict of interest

Authors LH, YW, CW, and ZL were employed by the company SINOPEC Corp. Author ZX was employed by the company China Petrochemical Corporation (SINOPEC Group).

Publisher's note

References

Arrigo, R., Havecker, M., Schlogl, R., and Su, D. S. (2008). Dynamic surface rearrangement and thermal stability of nitrogen functional groups on carbon nanotubes. *Chem. Commun.* 1, 4891–4893. doi:10.1039/b812769g

Bi, R., Wang, Q., Miao, C., Feng, J., and Li, D. (2019). Pd/NiO/Al array catalyst for 2-ethylanthraquinone hydrogenation: Synergistic effect between Pd and NiO/Al support. *Catal. Lett.* 149, 1286–1296. doi:10.1007/s10562-019-02712-y

Bulushev, D. A., Zacharska, M., Shlyakhova, E. V., Chuvilin, A. L., Guo, Y., Beloshapkin, S., et al. (2016). Single isolated Pd^{2+} cations supported on N-doped carbon as active sites for hydrogen production from formic acid decomposition. *ACS Catal.* 6, 681–691. doi:10.1021/acscatal.5b02381

Cao, Y., Mao, S., Li, M., Chen, Y., and Wang, Y. (2017). Metal/porous carbon composites for heterogeneous catalysis: Old catalysts with improved performance promoted by n-doping. *ACS Catal.* 7, 8090–8112. doi:10.1021/acscatal.7b02335

Chen, S., Qi, P., Chen, J., and Yuan, Y. (2015). Platinum nanoparticles supported on N-doped carbon nanotubes for the selective oxidation of glycerol to glyceric acid in a base-free aqueous solution. *RSC Adv.* 5, 31566–31574. doi:10.1039/c5ra02112j

Cui, X., Surkus, A. E., Junge, K., Topf, C., Radnik, J., Kreyenschulte, C., et al. (2016). Highly selective hydrogenation of arenes using nanostructured ruthenium catalysts modified with a carbon-nitrogen matrix. *Nat. Commun.* 7, 11326. doi:10.1038/ncomms11326

Fu, P., Zhou, L., Sun, L., Huang, B., and Yuan, Y. (2017). Nitrogen-doped porous activated carbon derived from cocoon silk as a highly efficient metal-free electrocatalyst for the oxygen reduction reaction. *RSC Adv.* 7, 13383–13389. doi:10.1039/c7ra00433h

Hao, J., Long, Z., Sun, L., Zhan, W., Wang, X., and Han, X. (2021). Hierarchical CeO_2@N-C ultrathin nanosheets for efficient selective oxidation of benzylic alcohols in water. *Inorg. Chem.* 60, 7732–7737. doi:10.1021/acs.inorgchem.1c00076

He, L., Wang, Y., Gao, H., Liu, Z., and Xie, Z. (2021). Nitrogen doped carbon for Pd-catalyzed hydropurification of crude terephthalic acid: Roles of nitrogen species. *RSC Adv.* 11, 33646–33652. doi:10.1039/d1ra06479g

Hu, H., Wang, J. J., Cui, B. F., Zheng, X. R., Lin, J. G., Deng, Y. D., et al. (2022). Atomically dispersed selenium sites on nitrogen-doped carbon for efficient electrocatalytic oxygen reduction. *Angew. Chem. Int. Ed. Engl.* 61, e202114441. doi:10.1002/anie.202114441

Jhung, S. H., Romanenko, A. V., Lee, K. H., Park, Y. S., Moroz, E. M., and Likholobov, V. A. (2002). Carbon-supported palladium-ruthenium catalyst for hydropurification of terephthalic acid. *Appl. Catal. A General* 225, 131–139. doi:10.1016/S0926-860X(01)00853-5

Jia, W., Zhang, M., Li, X., Zhang, Y., Meng, C., Tian, F., et al. (2021). Nitrogen-doped porous carbon-encapsulated copper composite for efficient reduction of 4-nitrophenol. *J. Colloid Interface Sci.* 594, 254–264. doi:10.1016/j.jcis.2021.03.020

Jiang, H., Yu, X., Nie, R., Lu, X., Zhou, D., and Xia, Q. (2016). Selective hydrogenation of aromatic carboxylic acids over basic N-doped mesoporous carbon supported palladium catalysts. *Appl. Catal. A General* 520, 73–81. doi:10.1016/j.apcata.2016.04.009

Kan, Y., Li, K., Wang, J., Lin, L., and Zeng, C. (2012). Preparation and characterization of TiO_2 support for Pd catalysts: Application in hydrogenation of 4-carboxybenzaldehyde. *Adv. Mat. Res.* 361-363, 584–592. doi:10.4028/www.scientific.net/amr.361-363.584

Li, J., Liu, J., Zhou, H., and Fu, Y. (2016a). Catalytic transfer hydrogenation of furfural to furfuryl alcohol over nitrogen-doped carbon-supported iron catalysts. *ChemSusChem* 9, 1339–1347. doi:10.1002/cssc.201600089

Li, K. T., Hsu, M. H., and Wang, I. (2008). Palladium core-porous silica shell-nanoparticles for catalyzing the hydrogenation of 4-carboxybenzaldehyde. *Catal. Commun.* 9, 2257–2260. doi:10.1016/j.catcom.2008.05.012

Li, M., Xu, F., Li, H., and Wang, Y. (2016b). Nitrogen-doped porous carbon materials: Promising catalysts or catalyst supports for heterogeneous hydrogenation and oxidation. *Catal. Sci. Technol.* 6, 3670–3693. doi:10.1039/C6CY00544F

Li, X., Tie, K., Li, Z., Guo, Y., Liu, Z., Liu, X., et al. (2018). Nitrogen-doped hierarchically porous carbon derived from cherry stone as a catalyst support for purification of terephthalic acid. *Appl. Surf. Sci.* 447, 57–62. doi:10.1016/j.apsusc.2018.03.195

Li, X., Zhao, S., Zhang, W., Liu, Y., and Li, R. (2016c). Ru nanoparticles supported on nitrogen-doped porous carbon derived from ZIF-8 as an efficient catalyst for the selective hydrogenation of p-chloronitrobenzene and p-bromonitrobenzene. *Dalton Trans.* 45, 15595–15602. doi:10.1039/c6dt02678h

Li, Z., Liu, J., Xia, C., and Li, F. W. (2013). Nitrogen-functionalized ordered mesoporous carbons as multifunctional supports of ultrasmall Pd nanoparticles for hydrogenation of phenol. *ACS Catal.* 3, 2440–2448. doi:10.1021/cs400506q

Liu, J., Du, W., Li, Z., and Yang, A. (2018). Preparation of TiO_2 nanotube supported Pd for the hydrogenation of 4-carboxy-benzaldehyde. *Catal. Lett.* 148, 2472–2479. doi:10.1007/s10562-018-2469-2

Liu, Y., He, Y., Zhou, D., Feng, J., and Li, D. (2016). Catalytic performance of Pd-promoted Cu hydrotalcite-derived catalysts in partial hydrogenation of acetylene: Effect of Pd-Cu alloy formation. *Catal. Sci. Technol.* 6, 3027–3037. doi:10.1039/c5cy01516b

Lobiak, E. V., Kuznetsova, V. R., Makarova, A. A., Okotrub, A. V., and Bulusheva, L. G. (2020). Structure, functional composition and electrochemical properties of nitrogen-doped multi-walled carbon nanotubes synthesized using Co-Mo, Ni-Mo and Fe-Mo catalysts. *Mat. Chem. Phys.* 255, 123563. doi:10.1016/j.matchemphys.2020.123563

Lu, C., Zhu, Q., Zhang, X., Ji, H., Zhou, Y., Wang, H., et al. (2019). Decoration of Pd nanoparticles with N and S doped carbon quantum dots as a robust catalyst for the chemoselective hydrogenation reaction. *ACS Sustain. Chem. Eng.* 7, 8542–8553. doi:10.1021/acssuschemeng.9b00322

Mao, S., Wang, C., and Wang, Y. (2019). The chemical nature of N doping on N doped carbon supported noble metal catalysts. *J. Catal.* 375, 456–465. doi:10.1016/j.jcat.2019.06.039

Menegazzo, F., Fantinel, T., Signoretto, M., and Pinna, F. (2007). Metal dispersion and distribution in Pd-based PTA catalysts. *Catal. Commun.* 8, 876–879. doi:10.1016/j.catcom.2006.09.021

Nagpure, A. S., Gurrala, L., Gogoi, P., and Chilukuri, S. V. (2016). Hydrogenation of cinnamaldehyde to hydrocinnamaldehyde over Pd nanoparticles deposited on nitrogen-doped mesoporous carbon. *RSC Adv.* 6, 44333–44340. doi:10.1039/c6ra04154j

Nie, R., Jiang, H., Lu, X., Zhou, D., and Xia, Q. (2016). Highly active electron-deficient Pd clusters on N-doped active carbon for aromatic ring hydrogenation. *Catal. Sci. Technol.* 6, 1913–1920. doi:10.1039/C5CY01418B

Peng, H., Liu, F., Liu, X., Liao, S., You, C., Tian, X., et al. (2014). Effect of transition metals on the structure and performance of the doped carbon catalysts derived from polyaniline and melamine for ORR application. *ACS Catal.* 4, 3797–3805. doi:10.1021/cs500744x

Podyacheva, O. Y., Cherepanova, S. V., Romanenko, A. I., Kibis, L. S., Svintsitskiy, D. A., Boronin, A. I., et al. (2017). Nitrogen doped carbon nanotubes and nanofibers: Composition, structure, electrical conductivity and capacity properties. *Carbon* 122, 475–483. doi:10.1016/j.carbon.2017.06.094

Quílez-Bermejo, J., Melle-Franco, M., San-Fabián, E., Morallón, E., and Cazorla-Amorós, D. (2019). Towards understanding the active sites for the ORR in N-doped carbon materials through fine-tuning of nitrogen functionalities: An experimental and computational approach. *J. Mat. Chem. A Mat.* 7, 24239–24250. doi:10.1039/c9ta07932g

Radkevich, V. Z., Senko, T. L., Wilson, K., Grishenko, L. M., Zaderko, A. N., and Diyuk, V. Y. (2008). The influence of surface functionalization of activated carbon on palladium dispersion and catalytic activity in hydrogen oxidation. *Appl. Catal. A General* 335, 241–251. doi:10.1016/j.apcata.2007.11.029

Shen, C., Jie, S., Chen, H., and Liu, Z. (2019). The Co-N-C catalyst synthesized with a hard-template and etching method to achieve well-dispersed active sites for ethylbenzene oxidation. *Front. Chem.* 7, 426. doi:10.3389/fchem.2019.00426

Shen, Q., Li, X., Li, R., and Wu, Y. (2020). Application of metal-organic framework materials and derived porous carbon materials in catalytic hydrogenation. *ACS Sustain. Chem. Eng.* 8, 17608–17621. doi:10.1021/acssuschemeng.0c06849

Shi, Z., Yang, W., Gu, Y., Liao, T., and Sun, Z. (2020). Metal-nitrogen-doped carbon materials as highly efficient catalysts: Progress and rational design. *Adv. Sci.* 7, 2001069. doi:10.1002/advs.202001069

Siuzdak, K., Szkoda, M., Sawczak, M., and Lisowska-Oleksiak, A. (2015). Novel nitrogen precursors for electrochemically driven doping of titania nanotubes exhibiting enhanced photoactivity. *New J. Chem.* 39, 2741–2751. doi:10.1039/c5nj00127g

Sun, Y., Chen, L., Bao, Y., Wang, G., Zhang, Y., Fu, M., et al. (2017). Roles of nitrogen species on nitrogen-doped CNTs supported Cu-ZrO_2 system for carbon dioxide hydrogenation to methanol. *Catal. Today* 307, 212–223. doi:10.1016/j.cattod.2017.04.017

Tie, K., Pan, X., He, L., Li, P., Yu, T., and Bao, X. (2018). Pd supported on NC@SiC as an efficient and stable catalyst for 4-carboxybenzaldehyde hydrogenation. *Catal. Commun.* 110, 79–82. doi:10.1016/j.catcom.2018.03.008

von Deak, D., Singh, D., King, J. C., and Ozkan, U. S. (2012). Use of carbon monoxide and cyanide to probe the active sites on nitrogen-doped carbon catalysts for oxygen reduction. *Appl. Catal. B Environ.* 113-114, 126–133. doi:10.1016/j.apcatb.2011.11.029

Wang, B., Zhao, J., Yue, Y., Sheng, G., Lai, H., Rui, J., et al. (2019). Carbon with surface-enriched nitrogen and sulfur supported au catalysts for acetylene hydrochlorination. *ChemCatChem* 11, 201801555–201811009. doi:10.1002/cctc.201801555

Wang, H., Jia, J., Song, P., Wang, Q., Li, D., Min, S., et al. (2017). Efficient electrocatalytic reduction of CO_2 by nitrogen-doped nanoporous carbon/carbon nanotube membranes: A step towards the electrochemical CO_2 refinery. *Angew. Chem. Int. Ed. Engl.* 56, 7955–7960. doi:10.1002/ange.201703720

Wang, Q., Zhao, J., Xu, L., Yu, L., Yao, Z., Lan, G., et al. (2021). Tuning electronic structure of palladium from wheat flour-derived N-doped mesoporous carbon for

efficient selective hydrogenation of acetylene. *Appl. Surf. Sci.* 562, 150141. doi:10.1016/j.apsusc.2021.150141

Wang, W., Yang, G., Wang, Q., Cao, Y., Wang, H., and Yu, H. (2022). Modifying carbon nanotubes supported palladium nanoparticles via regulatingthe electronic metal-carbon interaction for phenol hydrogenation. *Chem. Eng. J.* 436, 131758. doi:10.1016/j.cej.2021.131758

Wang, Z., Wei, J., Liu, G., Zhou, Y., Han, K., and Ye, H. (2015). G-C_3N_4-coated activated carbon-supported Pd catalysts for 4-CBA hydrogenation: Effect of nitrogen species. *Catal. Sci. Technol.* 5, 3926–3930. doi:10.1039/c5cy00625b

Warczinski, L., Hu, B., Eckhard, T., Peng, B., Muhler, M., and Hattig, C. (2020). Anchoring of palladium nanoparticles on N-doped mesoporous carbon. *Phys. Chem. Chem. Phys.* 22, 21317–21325. doi:10.1039/D0CP03234D

Wood, K. N., O'Hayre, R., and Pylypenko, S. (2014). Recent progress on nitrogen/carbon structures designed for use in energy and sustainability applications. *Energy Environ. Sci.* 7, 1212–1249. doi:10.1039/c3ee44078h

Xiong, H., Moyo, M., Motchelaho, M. A., Tetana, Z. N., Dube, S. M. A., Jewell, L. L., et al. (2014). Fischer-Tropsch synthesis: Iron catalysts supported on N-doped carbon spheres prepared by chemical vapor deposition and hydrothermal approaches. *J. Catal.* 311, 80–87. doi:10.1016/j.jcat.2013.11.007

Xu, X., Li, Y., Gong, Y., Zhang, P., Li, H., and Wang, Y. (2012). Synthesis of palladium nanoparticles supported on mesoporous N-doped carbon and their catalytic ability for biofuel upgrade. *J. Am. Chem. Soc.* 134, 16987–16990. doi:10.1021/ja308139s

Yang, J., Jo, M. R., Kang, M., Huh, Y. S., Jung, H., and Kang, Y. M. (2014). Rapid and controllable synthesis of nitrogen doped reduced graphene oxide using microwave-assisted hydrothermal reaction for high power-density supercapacitors. *Carbon* 73, 106–113. doi:10.1016/j.carbon.2014.02.045

Yang, J., Ju, Z., Jiang, Y., Xing, Z., Xi, B., Feng, J., et al. (2018). Enhanced capacity and rate capability of nitrogen/oxygen dual-doped hard carbon in capacitive potassium-ion storage. *Adv. Mat.* 30, 1700104. doi:10.1002/adma.201700104

Yu, H., Zhang, L., Gao, S., Wang, H., He, Z., Xu, Y., et al. (2021). *In situ* encapsulated ultrafine Pd nanoparticles in nitrogen-doped porous carbon derived from hyper-crosslinked polymers effectively catalyse hydrogenation. *J. Catal.* 396, 342–350. doi:10.1016/j.jcat.2021.03.002

Zhang, P., Sun, F., Xiang, Z., Shen, Z., Yun, J., and Cao, D. (2014). ZIF-derived *in situ* nitrogen-doped porous carbons as efficient metal-free electrocatalysts for oxygen reduction reaction. *Energy Environ. Sci.* 7 (1), 442–450. doi:10.1039/c3ee42799d

Zhou, Y. H., Li, X. Y., Pan, X. L., and Bao, X. H. (2012). A highly active and stable Pd-TiO_2/CDC-SiC catalyst for hydrogenation of 4-carboxybenzaldehyde. *J. Mat. Chem.* 22, 14155–14159. doi:10.1039/c2jm31503c

Zhou, Y., Li, L., Liu, Y., Wang, H., Feng, Z., Feng, F., et al. (2022). Palladium nanoparticles inset into the carbon sphere with robust acid resistance for selective hydrogenation of chloronitrobenzene. *Ind. Eng. Chem. Res.* 61, 4310–4319. doi:10.1021/acs.iecr.1c04983

Zhu, J., Wu, F., Li, M., Zhu, J., van Ommen, J. G., and Lefferts, L. (2015). Influence of internal diffusion on selective hydrogenation of 4-carboxybenzaldehyde over palladium catalysts supported on carbon nanofiber coated monolith. *Appl. Catal. A General* 498, 222–229. doi:10.1016/j.apcata.2015.03.036